THE PUBLISHING HOUSE
OF THE ROMANIAN ACADEMY

PROCEEDINGS OF THE ROMANIAN ACADEMY, Series A,
Volume 24, Number 2/2023, pp. 159–165
DOI: 10.59277/PRA-SER.A.24.2.08

ANALYTICAL METHOD FOR NONLINEAR MEMRISTIVE SYSTEMS

Bogdan MARINCA[1], Vasile MARINCA[1,2]

[1] Politehnica University Timişoara
[2] Center for Advanced and Fundamental Technical Research, Romanian Academy, Timişoara Branch
Bd. M. Viteazul Nr. 24, 300223, Timişoara România
Corresponding author: Bogdan MARINCA, e-mail: bogdan.marinca@upt.ro

Abstract. This work is devoted to providing an approximate analytical method to analyze memristor devices. One of basic property of the memristor is pinched hysteresis, considered to be a signature of the existence of memristance. The presence of hysteresis defines the material implementation of its memristive effects. This it its fundamental property, which looks more like a nonlinear anomaly. The memristor technology offers lower heat generation as it utilizes less energy. Optimal auxiliary functions method (OAFM) is implemented to find an approximate solution for the state variable in memristor with a very high accuracy. The presence of the auxiliary functions and some optimal convergence-control parameters C_i assure a fast convergence of the solutions.

***Key words**:* memristors, nonlinear drift, memristive devices, optimal auxiliary functions method.

1. INTRODUCTION

The memristor is known as a nonlinear resistor with memory or resistive random-access memory. The memristor was developed by Leon O. Chua in 1971 [1] when he was working in a lab at HP, trying to figure out crossbar switches but only in 2008, Strukov et al. [2] developed the practical model of a memristors. In the last years, this concept was extended to circuit elements with memory and to some memristive systems. The memristor is considered as the fourth class of electrical component after the familiar resistor, capacitor and inductor. One can consider that memristors maintain a relationship between the time integrals of voltage across and current through two terminals of an element, as they are passive circuit elements.

There are some applications of the memristors: logic circuits [3], neuromorphic circuit [4], artificial intelligence [5], coupled memristor and chaotic circuits [6] and so on.

Several works were carried out in the literature focused on numerical integration or approximate method: Finite Element Method [7], Volterra series [8], homotophy perturbation method [9], perturbation theory [10], homotophy analysis method [11], multiple scale [12].

In this paper we explore an approximate analytical solution for modelling of memristor device based on Joglekar and Wolf nonlinear window function [13]. Our approximate analytical solution for nonlinear systems is based upon original construction of the solutions using some auxiliary functions and a moderate number of optimal convergence-control parameters C_i. In comparison with any other methods known in literature, our technique led to a high accuracy via these parameters. OAFM is an iterative approach, which often rapidly converges to exact solution after only one iteration, is effective, explicit, simple and provides a rigorous way to control and adjust the convergence of the solutions. These observations are in fact the true power of our technique solving nonlinear problems without the presence of small or large parameters in the nonlinear differential equation or in the initial/boundary conditions.

2. MATHEMATICAL MODEL OF HP MEMRISTOR

In Fig. 1 is depicted HP memristor which has two platinum electrodes across a resistive material and its resistance depends on its polarity, magnitude and length. The resistance material can be titanium dioxide or

silicon dioxide. As voltage is applied across the terminals, the oxygen atoms within the material disperse toward one of the electrodes. This activity stretches or contracts the material depending on the polarity of the applied voltage, thereby changing the resistance of the memristor. The memristance of this example is a function of x, the extension of the doped titan oxide (TiO_{2-x}) region (high conductive) vs the non-doped titan oxide (TiO_2) region (low conductive).

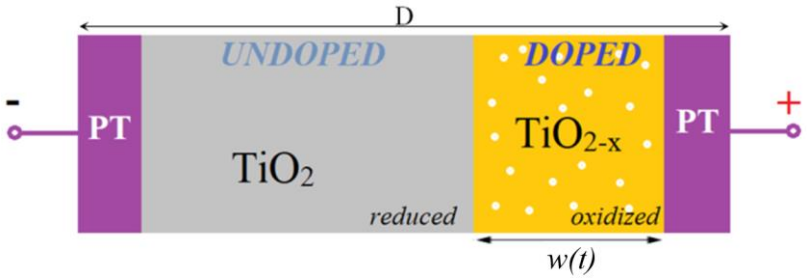

Fig. 1 – The memristance in this example is a function of $w(t)$, the extension of the doped titan dioxide (TiO_{2-x}) region vs the non-doped titan oxide (TiO_2) region (low conductive).

In this case the memristance, $[M]=\Omega$, is

$$M(t)=R_{\mathrm{ON}}\frac{w(t)}{D}+R_{\mathrm{OFF}}\left(1-\frac{w(t)}{D}\right) \tag{1}$$

or

$$M(t)=R_{\mathrm{OFF}}-\left(R_{\mathrm{OFF}}-R_{\mathrm{ON}}\right)x(t) \tag{2}$$

in which $x(t)$, $[x]=\mathrm{cm/cm}$, is the normalized state variable

$$x(t)=\frac{w(t)}{D},\quad x\in[0,1] \tag{3}$$

where R_{ON}, $[R_{\mathrm{ON}}]=\Omega$, and R_{OFF}, $[R_{\mathrm{OFF}}]=\Omega$, are limited values of the memristance for $w=D$, $[D]=\mathrm{cm}$, and $w=0$, respectively. $w(t)$ is the width of the doped domain and D is the whole length of the film. Taking into consideration the boundary nonlinear dopant drift, the variation of the state variable over time $\frac{\mathrm{d}x}{\mathrm{d}t}$ can be written as

$$\frac{\mathrm{d}x}{\mathrm{d}t}=kI(t)f_W(x),\quad k=\frac{\mu R_{\mathrm{ON}}}{D^2}, \tag{4}$$

where $I(t)$ is the electric current through the memristor, $[I]=\mathrm{A}$, k is proportionality factor, $[k]=\Omega\mathrm{s}^{-1}\mathrm{V}^{-1}$ and μ is average ionic mobility parameter $\mu=10^{-10}\mathrm{cm}^2\mathrm{s}^{-1}\mathrm{V}^{-1}$ and $f_w(x)$ is so-called window function. In our study, the window function is defined by Joglekar and Wolf function [13]

$$f_W(x)=1-(2x-1)^{2p} \tag{5}$$

where p is a positive integer number. The current through the memristor is defined by expression.

$$I(t)=A_0\sin\omega t \tag{6}$$

where A_0 is the electric current amplitude, $[A_0]=\mathrm{A}$, t is time, $[t]=\mathrm{s}$, and ω is the angular frequency of the current, $[\omega]=1/\mathrm{s}$.

From Eqs. (4), (5) and (6), the evolution of the state variable $x(t)$ is defined by nonlinear differential equation.

$$\frac{\mathrm{d}x}{\mathrm{d}t}=kA_0\sin\omega t\cdot\left[1-(2x-1)^{2p}\right] \tag{7}$$

In the following, we will solve Eq (7) by means of OAFM [14–17].

3. OAFM APPLIED TO HP MEMRISTOR

For nonlinear Eq (7) we consider the operators:

$$L\left[x(t)\right]=\frac{\mathrm{d}x}{\mathrm{d}t}(t);\quad N\left[x(t)\right]=-kA_0\sin\omega t\left[1-\left(2x-1\right)^{2p}\right], \tag{8}$$

where $[L]=1/\mathrm{s}$ and $[N]=1/\mathrm{s}$.

The initial approximation is determined from equation:

$$\frac{\mathrm{d}x_0}{\mathrm{d}t}(t)=0;\quad x_0(0)=\alpha, \tag{9}$$

whose solution is

$$x_0(t)=\alpha \tag{10}$$

The nonlinear operator N calculated for $x_0(t)$ becomes

$$N\left[x_0(t)\right]=kA_0\left[1-\left(2\alpha-1\right)^{2p}\right]\sin\omega t \tag{11}$$

The "source" functions for auxiliary functions F_j are obtained from Eqs (10) and (11) and therefore:

$$x_0(t)=\alpha,\quad N\left[x_0(t)\right]=C\sin j\omega t \tag{12}$$

The first approximation $x_1(t)$ is obtained from equation:

$$\frac{\mathrm{d}x_1}{\mathrm{d}t}\left(t,C_i\right)=\sum_{j=1}^{n}C_j\sin j\omega t,\quad x_1\left(0,C_i\right)=0 \tag{13}$$

such that one obtains:

$$x_1\left(t,C_i\right)=\frac{C_1}{\omega}\left(1-\cos\omega t\right)+\frac{C_2}{2\omega}\left(1-\cos 2\omega t\right)+\ldots+\frac{C_n}{n\omega}\left(1-\cos n\omega t\right) \tag{14}$$

where $[C_j]=1/\mathrm{s}$ and i and j are indices.

The approximate analytical solution of Eq (7) can be determined from Eqs (10) and (14):

$$\bar{x}(t)=\alpha+\frac{C_1}{\omega}\left(1-\cos\omega t\right)+\frac{C_2}{2\omega}\left(1-\cos 2\omega t\right)+\ldots+\frac{C_n}{n\omega}\left(1-\cos n\omega t\right) \tag{15}$$

4. NUMERICAL EXAMPLE

In this section, we consider that the parameters of this model are

$$\begin{gathered}R_{\mathrm{ON}}=100\ \Omega,\quad R_{\mathrm{OFF}}=16\cdot 10^{3}\Omega,\quad D=10^{-8}\mathrm{m},\\ k=10\ \Omega\mathrm{s}^{-1}\mathrm{V}^{-1},\quad A_0=4\ \mu\mathrm{A},\quad \omega=1\ \mathrm{s}^{-1},\quad \alpha=0.1\,.\end{gathered} \tag{16}$$

The validity of the OAFM is tested on two particular cases.

Case 4.1. In first case we consider $p=1$ into Joglekar-Wolf function (5) and $n=6$ into Eq. (15). The values of the optimal convergence-control parameters are obtained by means of the least square method:

$$\begin{gathered}C_1=0.016347269361;\quad C_2=-0.001004349645;\quad C_3=20.19000321\times10^{-5};\\ C_4=2.4253749776\times10^{-7};\quad C_5=-2.260559472\times10^{-8};\quad C_6=4.6525083756\times10^{-10}\end{gathered} \tag{17}$$

In this first case, the approximate analytical solution of Eq (7) for $p=1$ is

$$\bar{x}(t) = 0.115851880729316 - 0.01634726936\cos t + 0.000502174822542\cos 2t - \\ - 6.7300010690142\times 10^{-6}\cos 3t - 6.0634374444\times 10^{-8}\cos 4t + 4.521118944\times 10^{-9}\cos 5t - \\ - 7.75418062611\times 10^{-11}\cos 6t \tag{18}$$

Table 1

Comparison between the exact solution of Eq. (7) for $p = 1$ and approximate solution (18)

t (in seconds)	$x_{\text{exact}}(t)$	$\bar{x}(t)$ **Eq. (18)**	**Error** $\varepsilon = \lvert x_{\text{exact}} - \bar{x} \rvert$
0.25	0.100448552645	0.100448552626	2.6E–11
0.50	0.101776674045	0.1017766740165	1.6E–11
0.75	0.103930572087	0.1039305720537	5.7E–11
1.00	0.106817138429	0.10681713854712	1.5E–10
1.25	0.1103004166451	0.1103004166649	2.1E–11
1.50	0.114199733474	0.1141997332375	1.1E–10
1.75	0.118291956506	0.118291956398	1.0E–10
2.00	0.122320044811	0.1223200449082	1.1E–10
2.25	0.126008994212	0.1260089942224	2.2E–11
2.50	0.129088561815	0.1290885617187	8.1E–11
2.75	0.131320174387	0.1313201742944	5.5E–12
3.00	0.132523805342	0.132523805356	5.0E–12
π	0.132707989688	0.1327079897281	4.0E–11

Case 4.2. In the last case for $p = 2$ and $n = 6$ we obtain

$$\bar{x}(t) = 0.1264484431791 - 0.00737626947893\cos t + 0.0009161703712873\cos 2t + \\ + 1.2963742417198\times 10^{-5}\cos 3t - 1.286672990157\times 10^{-6}\cos 4t \\ - 2.392348037\times 10^{-8}\cos 5t + 2.703712706257\times 10^{-9}\cos 6t \tag{19}$$

In Tables 1 and 2 we present a comparison between the exact solution of Eq (7) and approximate solutions (18) and (19), respectively.

Table 2

Comparison between the exact solution of Eq. (7) for $p = 2$ and approximate solution (19)

t (in seconds)	$x_{\text{exact}}(t)$	$\bar{x}(t)$ **Eq. (19)**	**Error** $\varepsilon = \lvert x_{\text{exact}} - \bar{x} \rvert$
0.25	0.100736033597655	0.1007360335732	1.8E–11
0.50	0.102919984471032	0.10291998440004	7.1E–11
0.75	0.106475488317823	0.1064754881621	8.2E–11
1.00	0.111263723162145	0.111263723005295	1.6E–10
1.25	0.117071083637392	0.11707108361979	1.7E–11
1.50	0.123600941775782	0.12360094172872	4.7E–11
1.75	0.1304758875345	0.130475887194	3.4E–10
2.00	0.137254799255	0.137254799084	2.7E–10
2.25	0.143465113288917	0.143465113222	6.7E–11
2.50	0.148646196653278	0.14864619687	2.2E–10
2.75	0.152390638632141	0.1523296638976	3.4E–10
3.00	0.154417546590432	0.154417546566	2.4E–11
π	0.154726659322	0.154726659153	1.7E–10

The exact solution of Eq. (7) for $p=1$ and $p=2$ are obtained by integration.

It can be seen that the results by OAFM are of the very high accuracy in comparison with the exact solutions.

5. STUDY OF THE MEMRISTOR BY MEANS OF OAFM

Because the fast convergence of the OAFM, we will use the results obtained in Eqs. (18) and (19) for $p=1$ and $p=2$, respectively in the study of the memristor.

The hysteresis loop in Fig. 2 shows its switching characteristics: the memristance can switch between high resistance and low resistance. In the case of a positive voltage (the first quadrant), the state variable x increases and the memristance $M\left(x(t)\right)$ decreases. Follows that the current "on the way back" is large that on the "way up". But for a negative voltage, the state variable x decreases and the memristance increases and therefore resulting current decreases. The memristor retains a memory of its own past because that the same voltage can yield two different currents for a sinusoidal input current a given voltage can correspond to some different values of the current. The results are obtained from Eqs. (2), (18) (19), (6) and from the equations

$$U(t)=M\left[x(t)\right]I(t);\quad q=A_0\left(1-\cos\omega t\right);\quad \cos\omega t=\pm\sqrt{1-\frac{I^2}{{A_0}^2}}\quad\Rightarrow\quad q=A_0\left(1\pm\sqrt{1-\frac{I^2}{{A_0}^2}}\right) \tag{20}$$

where U is voltage, $[U]=\mathrm{V}$, and q is electric charge: $\dfrac{\mathrm{d}q(t)}{\mathrm{d}t}=I(t)$, $[q]=\mathrm{C}$.

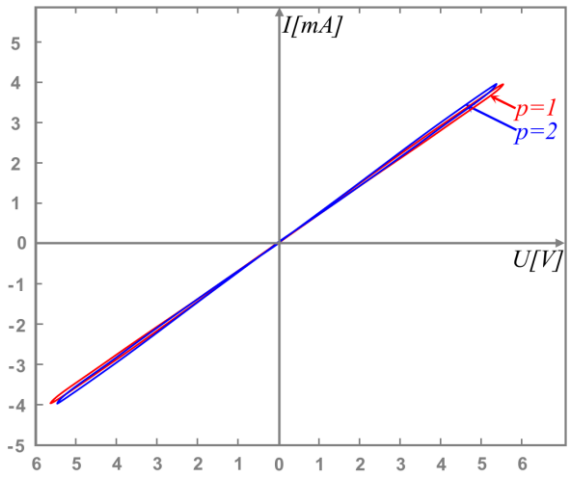

Fig. 2 – Relation between current I and voltage U.

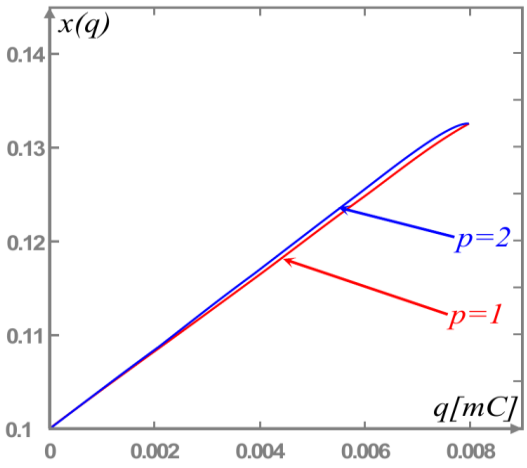

Fig. 3 – The state variable in respect to electric charge.

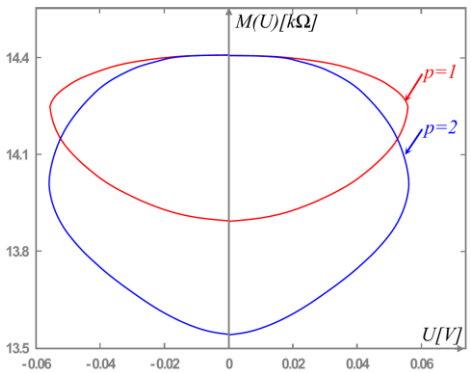

Fig. 4 – Relationships between the memristance and the voltage.

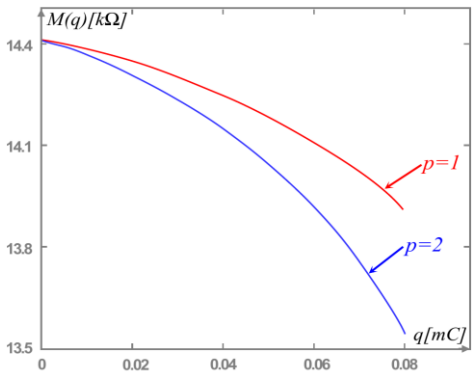

Fig. 5 – Relationships between the memristance and the electric charge.

The state variable is depicted in Fig. 3. The state variable increases with the increase of the charge but increases with increases of *p*. Figures. 4 and 5 show the relationship between the memristance and voltage and charge respectively. From Fig. 5 it can deduce that as *p* decreases, the memristance increases. Also, it can observe that in part of the lower memristance, the charge ratio is high, while in part of the higher memristance the charge ratio is low.

6. CONCLUSIONS

This work is devoted to use a novel modeling methodology for memristor system using an approximate analytical technique to analyze memristor devices. The characteristics curves of the memristive behavior are incorporated in the memory of the memristor models. The drift of the dopant has been implemented by the improved window functions.

It is known that any numerical procedure presents error [19] as local truncation or total accumulated errors, and these problems constitute a great obstacle in view of simulation design or analysis of the memristor. But OAFM eliminates the errors occurring in the simulation of some existing window functions. OAFM is capable of generating memristor models, the results obtained show that the pinched hysteresis loop with use of OAFM and Joglekar window functions transmitted to the input-output transfer characteristics. The most important advantage of our technique is that the formula of the memristance is given.

OAFM is an iterative procedure which rapidly converges to exact solution after only one approximation. Our procedure led to a very high accuracy is effective, explicit, simple and provides a rigorous with to control and adjust the convergence of the solutions.

The derived analysis can provide a basis to identify and model the memristor in a simple and convenient way which could help the researchers to analyse memristors and memristive systems. The results presented in this work show that our technique represents a significant improvement over existing technique.

REFERENCES

1. L.O. CHUA, *Memristors the missing circuit element*, IEEE Transactions on Circuits and System, **18**, pp. 507–519, 1971.
2. D.B. STRUKOV, G.S. SNIDER, D.R. STEWART, R.S. WILLIAMS, *The missing memristor found*, Nature, **453**, *191*, pp. 80–83, 2008.
3. L. GUCKERT, E.E. SWARTZLANDER JR, *MAD gates – memristor logic design using driven circuit*, IEEE Trans. Circuits Syst. II Exp. Briefs, **64**, *2*, pp. 171–175, 2017.
4. S.H. JO, T. CHANG, I. EBONG, B.B. BHADVYA, P. MAMZUDER, W. LU, *Nanoscale memristor device as synapse in neuromorphic systems*, Nano Lett., **10**, *4*, pp 1297–1301, 2010.
5. V. MILO, D. IELMINI, E. CHICCA, *Attractor network and associative memories with STDP learning in RRAM synapses*, 2017 IEEE International Electron Devices Meeting (IEDM), San Francisco, CA, USA, 2017, fasc. 7, pp. 1121–1124.
6. D.S. YU, H.H.C. IU, Y. LIANG, T. FERNANDO, L.O. CHUA, *Dynamic behavior of complex memristor circuits*, IEEE Trans. Circuits Syst. I, Reg. Papers, **62**, *6*, pp. 1607–1616, 2015.
7. I. MESSARIS, A. SERB, S. STATHOPOULOS, A. KHIAT, S. NICOLAIDIS, T. PRODROMAKIS, *A data-driven Veriolog – A Re RAM model*, IEEE Trans. Comput. Aided Des. Integr. Circuits Syst., **37**, *12*, pp. 3151–3162, 2018.
8. A. ASCOLI, R. TETZLAFF, *Analytical model for ideal generic memristor circuits based on the theory of Volterra*, Proc. GMM/ITG/GI Symp. Rel. Design, 2015.
9. C.H. MEJIA, A.S. REYES, H.V. LEAL, *A novel modelling methodology for memristive systems using homotophy perturbation methods*, Circuits Syst. Signal Procrss , 36, pp. 947–968, 2017, DOI: 10.1007/s00034-016-0346-z.
10. S.C. YENER, R. MUTLU, H.H. KUNTMAN, *Small signal analysis of memristor-based low-pass and high-pass filters using the perturbation theory*, Optoelectronics and Advanced materials – Rapid communications, **12**, *1–2*, pp. 55–62, 2018.
11. W. HU, H. LUO, C. CHEN, R. WEI, *An analytic HAM-based modelling methodology for memristor enabling fast convergence*, https//arxiv.org/abs/1812.00317, 2018.
12. J.K. CHANDIA, M. BOLOGNA, B. TELLINI, *Multiple scale approach to dynamics of an LC circuit with a charge-controlled memristor*, IEEE Trans. Circuits Syst. II Express Briefs, **65**, *1*, pp. 120–124, 2018.
13. Y.A. JOGLEKAR, S.J. WOLF, *The elusive memristor properties of basic electrical circuits*, European Journal of Physics, **30**, *4*, pp. 661–675, 2009.
14. V. MARINCA, N. HERIŞANU, *Vibration on nonlinear nonlocal elastic column with initial imperfection*, Acoustics and Vibration of Mechanical Structures AVMS-2017, Springer Proceedings in Physics, **198**, pp. 49–56, 2018.

15. B. MARINCA, V. MARINCA, *Approximate analytical solution for thin film flow of a fourth-grade fluid down a vertical cylinder*, Proceedings of the Romanian Academy, Series A, **19**, *1*, pp. 69–76, 2018.
16. V. MARINCA, R. D. ENE, B. MARINCA, *Optimal auxiliary functions method for viscous flow due to a stretching surface with partial slip*, Open Eng., **8**, pp. 261–274, 2018.
17. N. HERIŞANU, V. MARINCA, GH. MADESCU, F. DRĂGAN, *Dynamic response of a permanent magnet synchronous generator to a wind gust*, Energies, **12**, art. 915, 2019.
18. V. MARINCA, N. HERIŞANU, *The optimal homotopy asymptotic method*, Springer, 2015.
19. L.D. CHUA, P.X. LIN, *Computer aided analysis in electric circuits: Algorithms and computational techniques*, Prentice Hall Profesional Technical Reference, 1975.

Received December 7, 2022